SUPPLEMENTARY INFORMATION

Atomic structures of an entire contractile injection system in both the extended and contracted states

Ambroise Desfosses, Hariprasad Venugopal, Tapan Joshi, Jan Felix, Matthew Jessop, Hyengseop Jeong, Jaekyung Hyun, J. Bernard Heymann, Mark R. H. Hurst *, Irina Gutsche *, Alok K. Mitra *

*: corresponding author

Supplementary Figures 1 to 9

Supplementary Tables 1 to 6

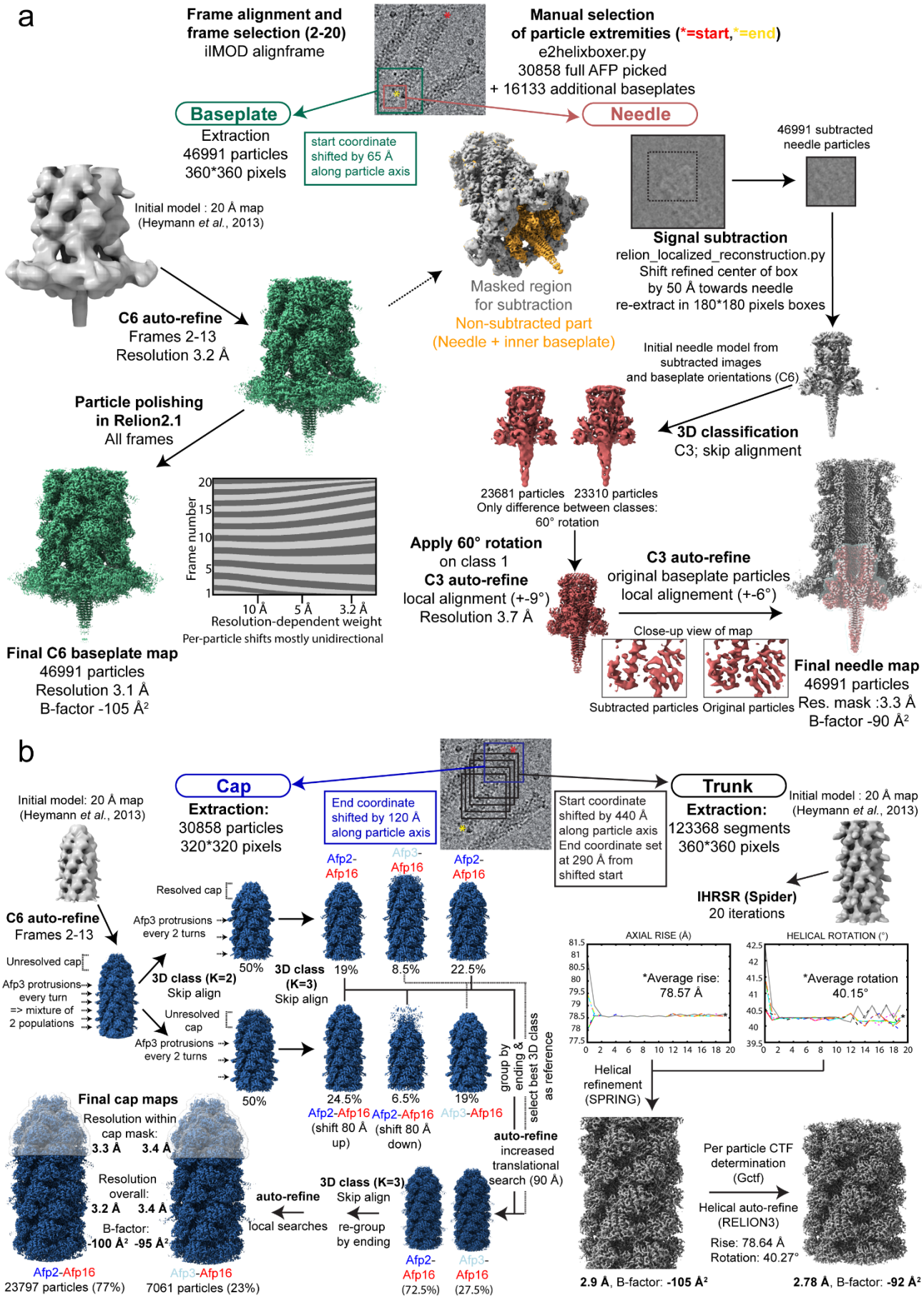
a
Frame alignment and frame selection (2-20)
iIMOD alignframe
Manual selection of particle extremities (*=start,*=end)
e2helixboxer.py
30858 full AFP picked
+ 16133 additional baseplates
Baseplate
Extraction
46991 particles
360*360 pixels
start coordinate shifted by 65 Å along particle axis
Needle
46991 subtracted needle particles
Initial model : 20 Å map (Heymann et al., 2013)
Masked region for subtraction
Non-subtracted part (Needle + inner baseplate)
Signal subtraction
relion_localized_reconstruction.py
Shift refined center of box by 50 Å towards needle
re-extract in 180*180 pixels boxes
C6 auto-refine
Frames 2-13
Resolution 3.2 Å
Initial needle model from subtracted images and baseplate orientations (C6)
Particle polishing in Relion2.1
All frames
3D classification
C3; skip alignment
23681 particles
23310 particles
Only difference between classes: 60° rotation
Frame number
Resolution-dependent weight
Per-particle shifts mostly unidirectional
Apply 60° rotation
on class 1
C3 auto-refine
local alignment (+-9°)
Resolution 3.7 Å
C3 auto-refine
original baseplate particles
local alignement (+-6°)
Close-up view of map
Subtracted particles
Original particles
Final C6 baseplate map
46991 particles
Resolution 3.1 Å
B-factor -105 Å²
Final needle map
46991 particles
Res. mask :3.3 Å
B-factor -90 Å²
b
Initial model: 20 Å map (Heymann et al., 2013)
Cap
Extraction:
30858 particles
320*320 pixels
End coordinate shifted by 120 Å along particle axis
Trunk
Extraction:
123368 segments
360*360 pixels
Start coordinate shifted by 440 Å along particle axis
End coordinate set at 290 Å from shifted start
Initial model : 20 Å map (Heymann et al., 2013)
IHRSR (Spider)
20 iterations
C6 auto-refine
Frames 2-13
Resolved cap
Afp3 protrusions every 2 turns
Unresolved cap
Afp3 protrusions every turn => mixture of 2 populations
3D class (K=2)
Skip align
50%
50%
3D class (K=3)
Skip align
Afp2-Afp16
Afp3-Afp16
Afp2-Afp16
19%
8.5%
22.5%
24.5%
6.5%
19%
Afp2-Afp16 (shift 80 Å up)
Afp2-Afp16 (shift 80 Å down)
Afp3-Afp16
group by ending & select best 3D class as reference
AXIAL RISE (Å)
*Average rise: 78.57 Å
HELICAL ROTATION (°)
*Average rotation 40.15°
Helical refinement (SPRING)
Final cap maps
Resolution within cap mask:
3.3 Å
3.4 Å
Resolution overall:
3.2 Å
3.4 Å
B-factor:
-100 Å²
-95 Å²
Afp2-Afp16
23797 particles (77%)
Afp3-Afp16
7061 particles (23%)
auto-refine
local searches
3D class (K=3)
Skip align
re-group by ending
auto-refine
increased translational search (90 Å)
Afp2-Afp16
(72.5%)
Afp3-Afp16
(27.5%)
Per particle CTF determination (Gctf)
Helical auto-refine (RELION3)
Rise: 78.64 Å
Rotation: 40.27°
2.9 Å, B-factor: -105 Å²
2.78 Å, B-factor: -92 Å²

Supplementary Figure 1: Flowcharts of the image processing pipeline for the AFP baseplate and needle (a), and apical cap and trunk (b) in the extended state. In the flowcharts, a representative micrograph is shown with boxed picked particles for the Baseplate (a, green), Needle (a, red), Cap (b, blue) and Trunk (b, black), followed by subsequent particle extraction, masking, signal subtraction, classification and refinement procedures performed in this study. At the bottom of each flowchart, final maps are shown with annotated overall resolution and b-factor. Used software packages are indicated where needed. For a full description of the image processing pipeline, see 'Methods'.

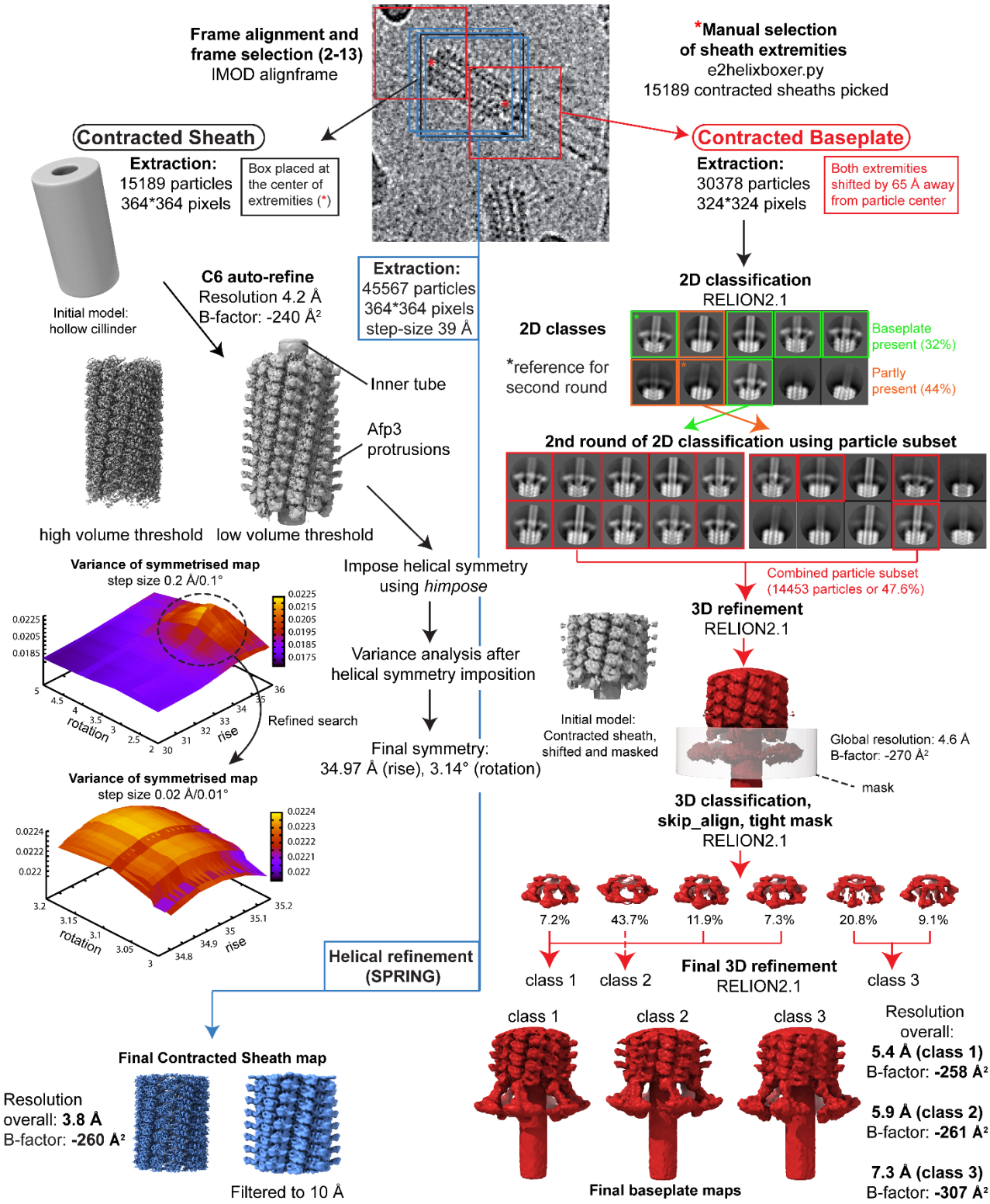
Frame alignment and frame selection (2-13)
IMOD alignframe
*Manual selection of sheath extremities
e2helixboxer.py
15189 contracted sheaths picked
Contracted Sheath
Extraction:
15189 particles
364*364 pixels
Box placed at the center of extremities (*)
Contracted Baseplate
Extraction:
30378 particles
324*324 pixels
Both extremities shifted by 65 Å away from particle center
Initial model:
hollow cillinder
C6 auto-refine
Resolution 4.2 Å
B-factor: -240 Å²
Extraction:
45567 particles
364*364 pixels
step-size 39 Å
2D classification
RELION2.1
2D classes
*reference for second round
Baseplate present (32%)
Partly present (44%)
Inner tube
Afp3 protrusions
2nd round of 2D classification using particle subset
high volume threshold
low volume threshold
Combined particle subset (14453 particles or 47.6%)
Impose helical symmetry using *himpose*
Variance of symmetrised map
step size 0.2 Å/0.1°
Variance analysis after helical symmetry imposition
3D refinement
RELION2.1
Initial model:
Contracted sheath, shifted and masked
Refined search
Final symmetry:
34.97 Å (rise), 3.14° (rotation)
Global resolution: 4.6 Å
B-factor: -270 Å²
mask
Variance of symmetrised map
step size 0.02 Å/0.01°
3D classification,
skip_align, tight mask
RELION2.1
7.2%
43.7%
11.9%
7.3%
20.8%
9.1%
Helical refinement (SPRING)
class 1
class 2
Final 3D refinement
RELION2.1
class 3
Final Contracted Sheath map
Resolution overall: 3.8 Å
B-factor: -260 Å²
Filtered to 10 Å
class 1
class 2
class 3
Final baseplate maps
Resolution overall:
5.4 Å (class 1)
B-factor: -258 Å²
5.9 Å (class 2)
B-factor: -261 Å²
7.3 Å (class 3)
B-factor: -307 Å²

Supplementary Figure 2: Flowchart of the image processing pipeline for the AFP sheath and baseplate in the contracted state. A representative micrograph is shown with boxed picked particles (black: Contracted Sheath start, blue: Contracted Sheath final, red: Contracted Baseplate), followed by subsequent particle extraction, masking, classification and refinement procedures performed in this study. At the bottom of the flowchart, final maps are shown with annotated overall resolution and b-factor. Used software packages are indicated where needed. For a full description of the image processing pipeline, see ’Methods’.

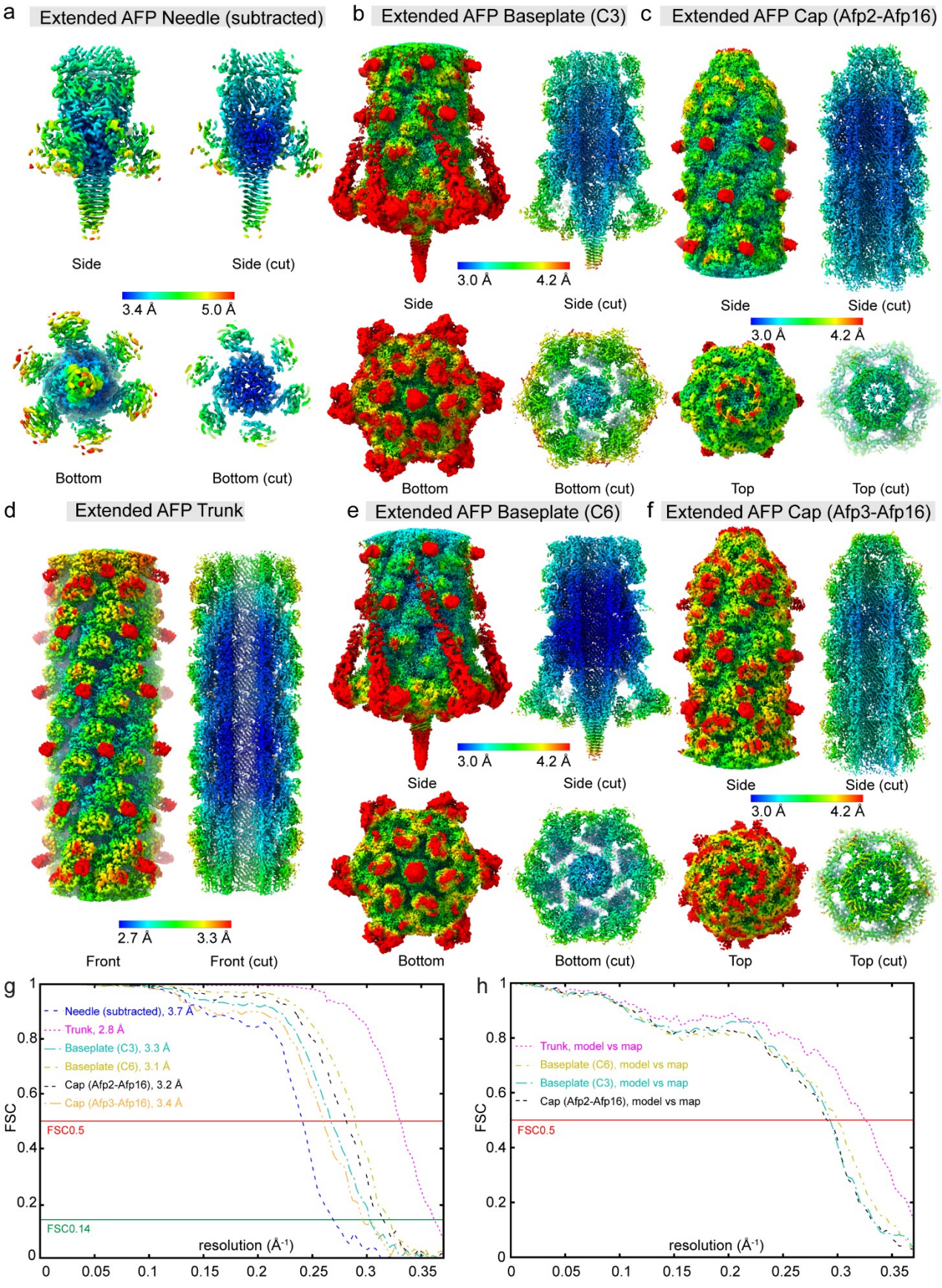
a
Extended AFP Needle (subtracted)
Side
Side (cut)
3.4 Å
5.0 Å
Bottom
Bottom (cut)
b
Extended AFP Baseplate (C3)
3.0 Å
4.2 Å
Side
Side (cut)
Bottom
Bottom (cut)
c
Extended AFP Cap (Afp2-Afp16)
Side
Side (cut)
3.0 Å
4.2 Å
Top
Top (cut)
d
Extended AFP Trunk
2.7 Å
3.3 Å
Front
Front (cut)
e
Extended AFP Baseplate (C6)
3.0 Å
4.2 Å
Side
Side (cut)
Bottom
Bottom (cut)
f
Extended AFP Cap (Afp3-Afp16)
Side
Side (cut)
3.0 Å
4.2 Å
Top
Top (cut)
g
Needle (subtracted), 3.7 Å
Trunk, 2.8 Å
Baseplate (C3), 3.3 Å
Baseplate (C6), 3.1 Å
Cap (Afp2-Afp16), 3.2 Å
Cap (Afp3-Afp16), 3.4 Å
FSC0.5
FSC0.14
FSC
resolution (Å-1)
0
0.2
0.4
0.6
0.8
1
0.05
0.1
0.15
0.2
0.25
0.3
0.35
h
Trunk, model vs map
Baseplate (C6), model vs map
Baseplate (C3), model vs map
Cap (Afp2-Afp16), model vs map
FSC0.5
FSC
resolution (Å-1)

Supplementary Figure 3: Gallery of unmasked cryo-EM maps, filtered and coloured by local resolution, and accompanying FSC curves for the extended AFP apical cap, trunk, baseplate and needle. Unmasked cryo-EM maps for the extended AFP needle (a), baseplate processed with C3 symmetry (b), cap terminating with Afp2-Afp16 (c), trunk (d), baseplate processed with C6 symmetry (e), and cap terminating with Afp3-Afp16 (f) filtered and coloured by local resolution. For panels b, c, d, e and f, contour levels (σ-values) used in Chimera to generate full and cut-out views are: full = 0.015 and cut-out = 0.07 (b), full = 0.02 and cut-out = 0.09 (c), full = 0.025 and cut-out = 0.08 (d), full = 0.015 and cut-out = 0.07 (e), full = 0.02 and cut-out = 0.09 (f). (g) Accompanying FSC curves for the maps shown in (a-f). In the legend, the resolution at the FSC cut-off of 0.5 (red) and 0.143 (green) is indicated. (f) Accompanying model vs map FCS curves for the extended AFP trunk, baseplate (C6), baseplate (C3) and cap. The resolution at the FSC cut-off of 0.5 is indicated in red.

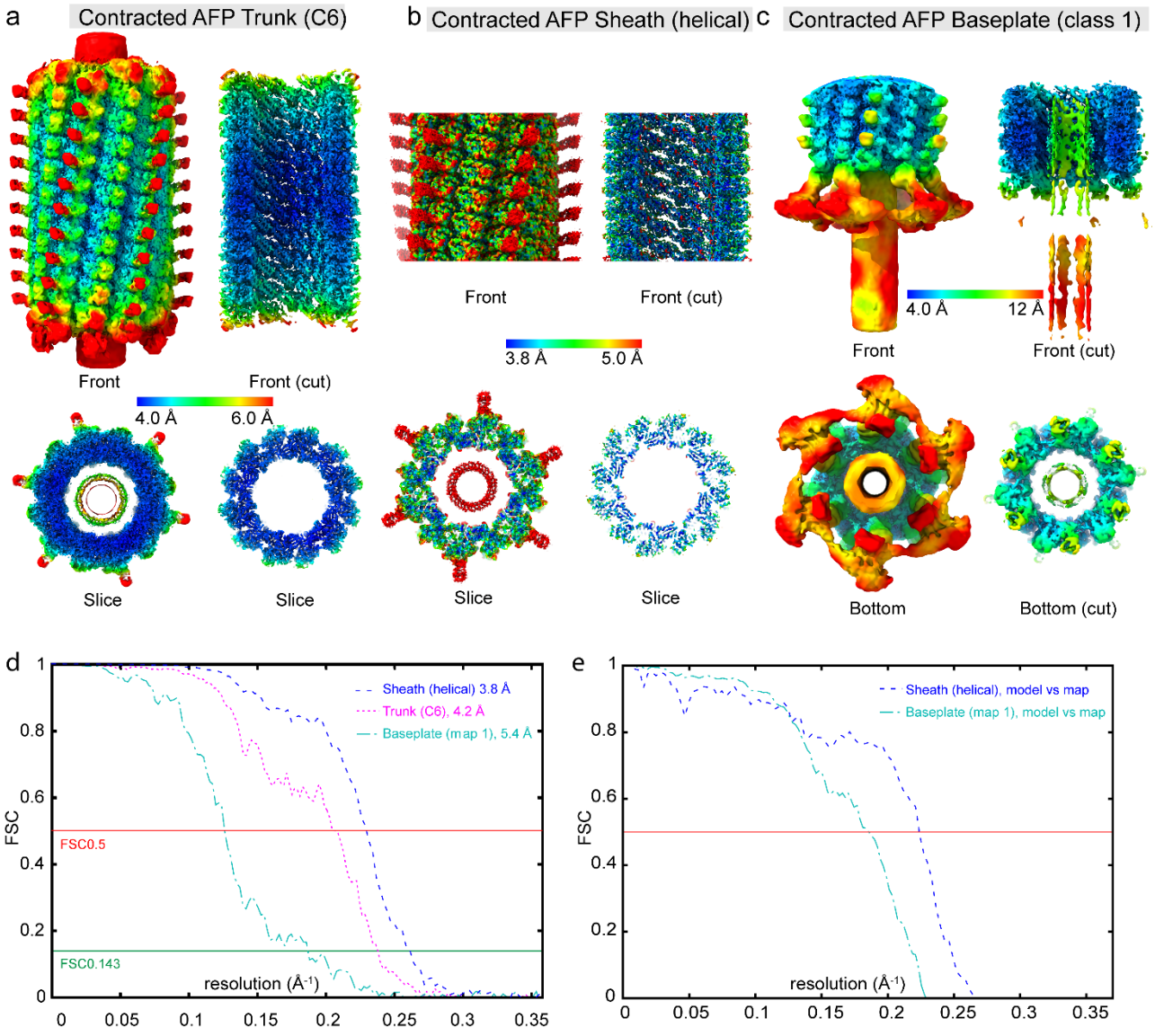

Supplementary Figure 4: Gallery of unmasked cryo-EM maps, filtered and coloured by local resolution, and accompanying FSC curves for the contracted AFP apical sheath and baseplate. Unmasked cryo-EM maps for the entire contracted AFP trunk processed with C6 symmetry (a), sheath processed with helical symmetry (b), and baseplate map 1 (c) filtered and coloured by local resolution. For panels a, b and c, the contour levels (σ-values) used in Chimera to generate full and cut-out views are: full = 0.035 and cut-out = 0.1 (a), full = 0.9 and cut-out = 2.5 (b), full = 0.03 and cut-out = 0.065 (c). (d) Accompanying FSC curves for the maps shown in a-c. In the legend, the resolution at the FSC cut-off of 0.5 (red) and 0.143 (green) is indicated. (f) Accompanying model vs map FCS curves for the contracted AFP helical sheath and baseplate. The resolution at the FSC cut-off of 0.5 is indicated in red.

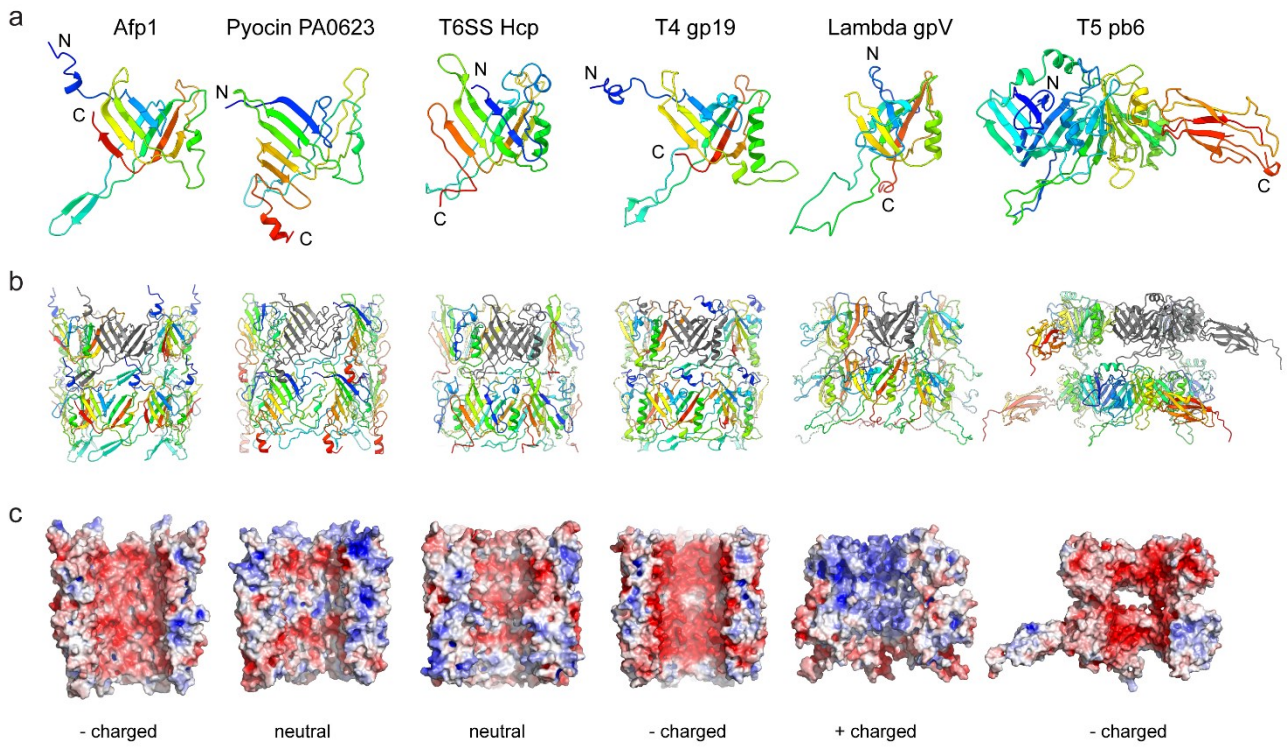

Supplementary Figure 5: Comparison of tube proteins for AFP (Afp1), Pyocin (PA0623), T6SS (Hcp), phage T4 (gp19), phage Lambda (gpV), and phage T5 (pb6). (a) Comparison of extracted monomers of Pyocin PA0623 (PDB ID: 5W5E) T6SS Hcp (PDB ID: 5OjQ), T4 gp19 (PDB ID: 5IV5), phage Lambda gpV (PDB ID: 2K4Q) and phage T5 pb6 (PDB ID: 5NGJ). Structures are shown as cartoons and coloured using a rainbow gradient with annotated N- and C-termini. (b) Double hexameric ring assemblies, corresponding to a 2-layer tube, formed by the tube proteins shown in (a). One monomer per tube is coloured dark grey. (c) Cut-out view of the hexameric ring assemblies shown in (b), coloured according to an electrostatic potential map calculated using APBS (Adaptive Poisson-Boltzmann Solver), where red and blue correspond to negative and positive charges respectively.

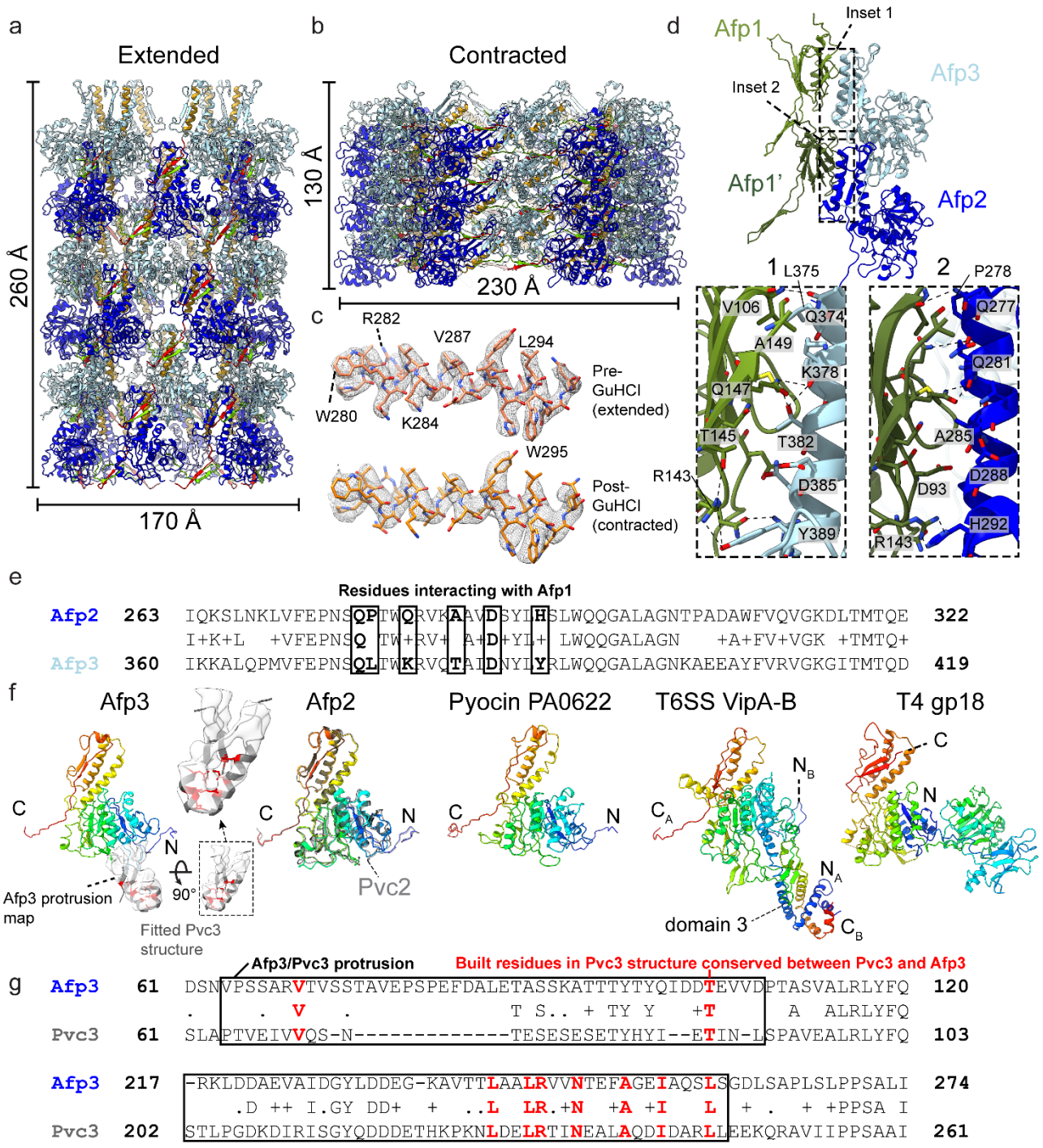

Supplementary Figure 6: Interactions between the extended AFP tube and sheath, and comparison with the contracted AFP state. (a-b) Structural organisation of Afp2 (dark blue) and Afp3 (light blue) in the extended (a) and contracted (b) AFP sheath. The β-strands from N and C-termini of Afp2 and Afp3, involved in the handshake (β-strand exchange) mechanism are coloured green (N-ter) and red (C-ter). The length of three layers of alternating Afp2/Afp3 rings is annotated for the extended (a) and contracted (b) AFP sheath. (c) Density for the α-helix spanning residues Proline 278 (P278) to Glutamine 297 (Q297) of Afp2 before (extended state) and after (contracted

state) addition of guanidinium chloride (GuHCL) is shown. Note the slightly disappearing density for residues Arginine 282 (R282), Lysine 284 (K284), Valine 287 (V287) and Leucine 294 (L294) after addition of GuHCL. (d) Interaction between two copies of Afp1 (light and dark green), Afp2 (dark blue) and Afp3 (light blue) in the AFP extended state. Inset 1 and 2 show a zoom of the interactions between Afp1 (light green) and Afp3 (light blue) and Afp1' (dark green) and Afp3 (dark blue) respectively. Structures are shown as cartoons while selected interacting residues are shown as sticks. H-bonds and electrostatic interactions are depicted using dotted black lines. (e) Sequence alignment between the α-helices spanning residues 263-322 of Afp2 and residues 360-419 of Afp3. Residues of Afp2/Afp3 interacting with Afp1 are annotated using black boxes. (f) Comparison between the sheath proteins from AFP (Afp2 and 3), PVC (Pvc2, PDB ID: 6J0B), Pyocin (PA0622, PDB ID: 3J9Q), T6SS (VipA and B, PDB ID: 3J9G) and phage T4 (gp18, PDB ID: 3J2M). Structures are shown as cartoons and coloured using a rainbow gradient, except for Pvc2 which is coloured grey, with annotated N- and C-termini. For Afp3, density is shown for the protrusion made up by two separate loops containing residues 65-105 and 215-265 (not modelled) in which the corresponding protrusion of Pvc3 is fitted (PDB ID: 6J0N). Conserved residues between Afp3 and Pvc3 in the protrusion domain are shown in red. (g) Sequence alignment between the protrusion domain of Afp3 and Pvc3. Conserved residues between Afp3 and Pvc3 are labelled in black, while conserved residues between Afp3 and Pvc3 which are present in the Pvc3 structure are labelled red. The split Afp3/Pvc3 protrusion domain is indicated by two black boxes.

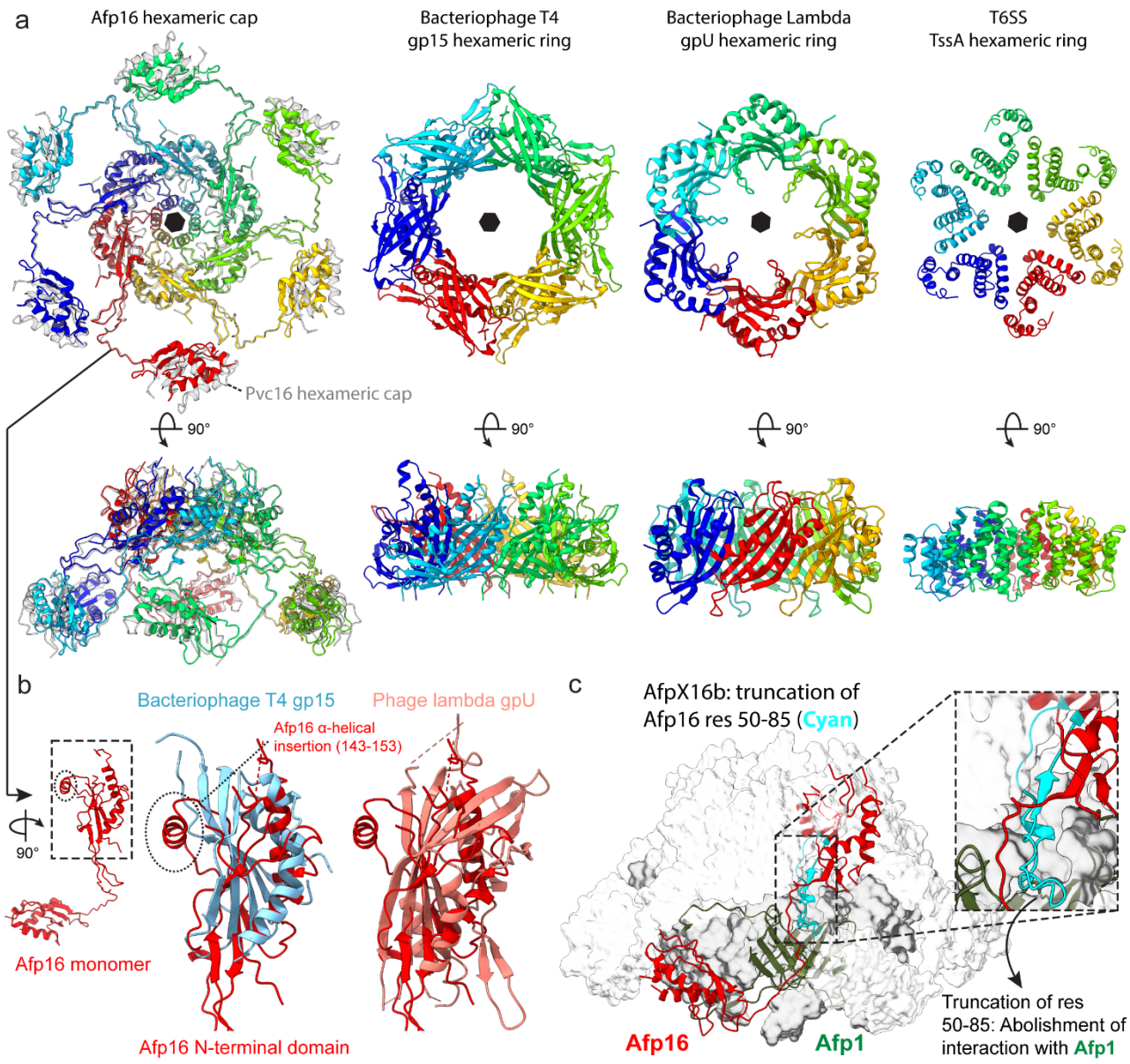

Supplementary Figure 7: Structural comparison between the AFP apical cap protein Afp16, the PVC apical cap protein Pvc16, and the tail terminator proteins gp15 from phage T4, gpU from phage Lambda and TssA from T6SS. (a) Top- (upper panels) and side-views (lower panels) of the hexameric cap formed by Afp16 aligned with the hexameric cap formed by Pvc16 (PDB ID: 6J0F), and hexameric rings formed by gp15 (PDB ID: 4HUH), gpU (PDB ID: 3FZB) and TssA (PDB ID: 4YO5). 6-fold rotation axes are indicated using black hexagons. (b) Structural alignment between the Afp16 N-terminal domain (red) and extracted monomers of phage T4 gp15 (light blue) and phage Lambda gpU (salmon). The α-helical insertion of Afp16 spanning residues 143-153 is annotated using a dotted black oval. (c) Position of Afp1 and Afp16 in the AFP extended state apical cap. One copy of Afp1 and Afp16 are shown as cartoons and coloured green and red respectively, while

remaining Afp1 and Afp16 copies are shown as a transparent white surface. Afp16 residues 50-85 (coloured light cyan) are absent in AfpX16b, the cap protein in the AFP variant AFP-X in *S. proeamaculans*□, thus leading to an abolished Afp1 interaction (see inset). This diminishes the capping capability of AfpX16b, resulting in greater variability in the lengths of AFP-X.

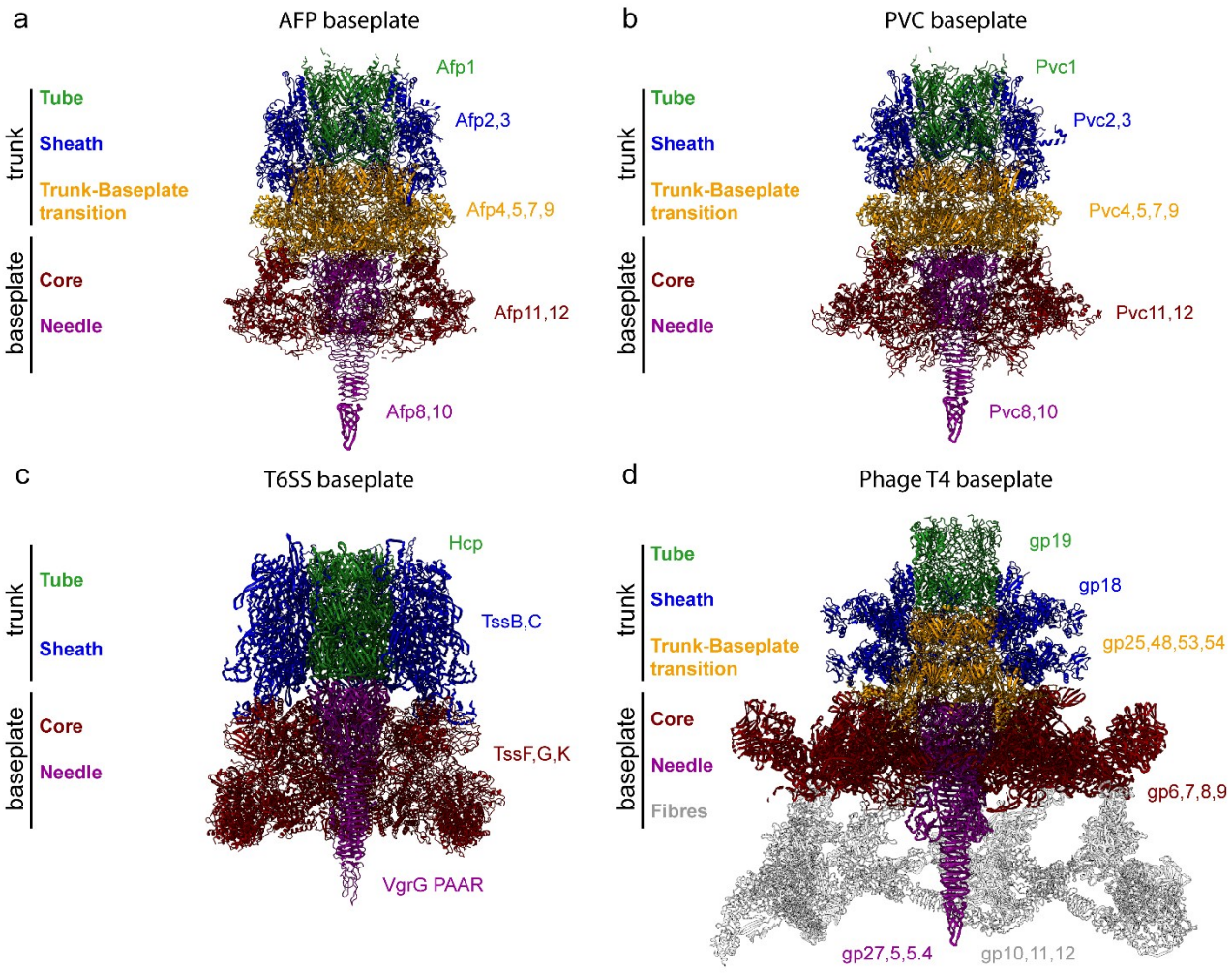

Supplementary Figure 8: Comparison between the overall architecture of AFP, PVC, T6SS and phage T4 baseplate structures. Cut-out front views of AFP (a), PVC (b), T6SS (c) and phage T4 (d) baseplate structures. For each structure, the first layers of the trunk are displayed. The individual proteins are coloured based on their position in the trunk (Tube: green, Sheath: blue, Trunk-Baseplate transition: orange) or baseplate (Core: red, Needle: purple and Fibres: transparent grey). Baseplate structures were generated as follows: For AFP and PVC, deposited structures of the respective baseplate (AFP: 6RAO, PVC: 6J0N) and needle (AFP: 6RBK, PVC: 6J0M) were combined with gp5.4 from phage T4, fitted in the AFP and PVC baseplate maps (AFP: EMD-4800, PVC: EMD-9764). For T4, the structure of the baseplate (PDB ID: 5IV5) and the structure of the sheath/tube (PDB ID: 3J2M), were fitted together in the cryo-EM reconstruction of the extended T4 tail (EMD-1126) to generate the full assembly. For T6SS, each subcomplex structure (Tube and sheath: PDB ID 5OJQ, Needle: PDB ID 4MTK and 4JIV, Core: PDB ID 6N38) was fitted into the cryo-EM reconstruction of the Vibrio Cholerae T6SS baseplate/needle (EMD-3879).

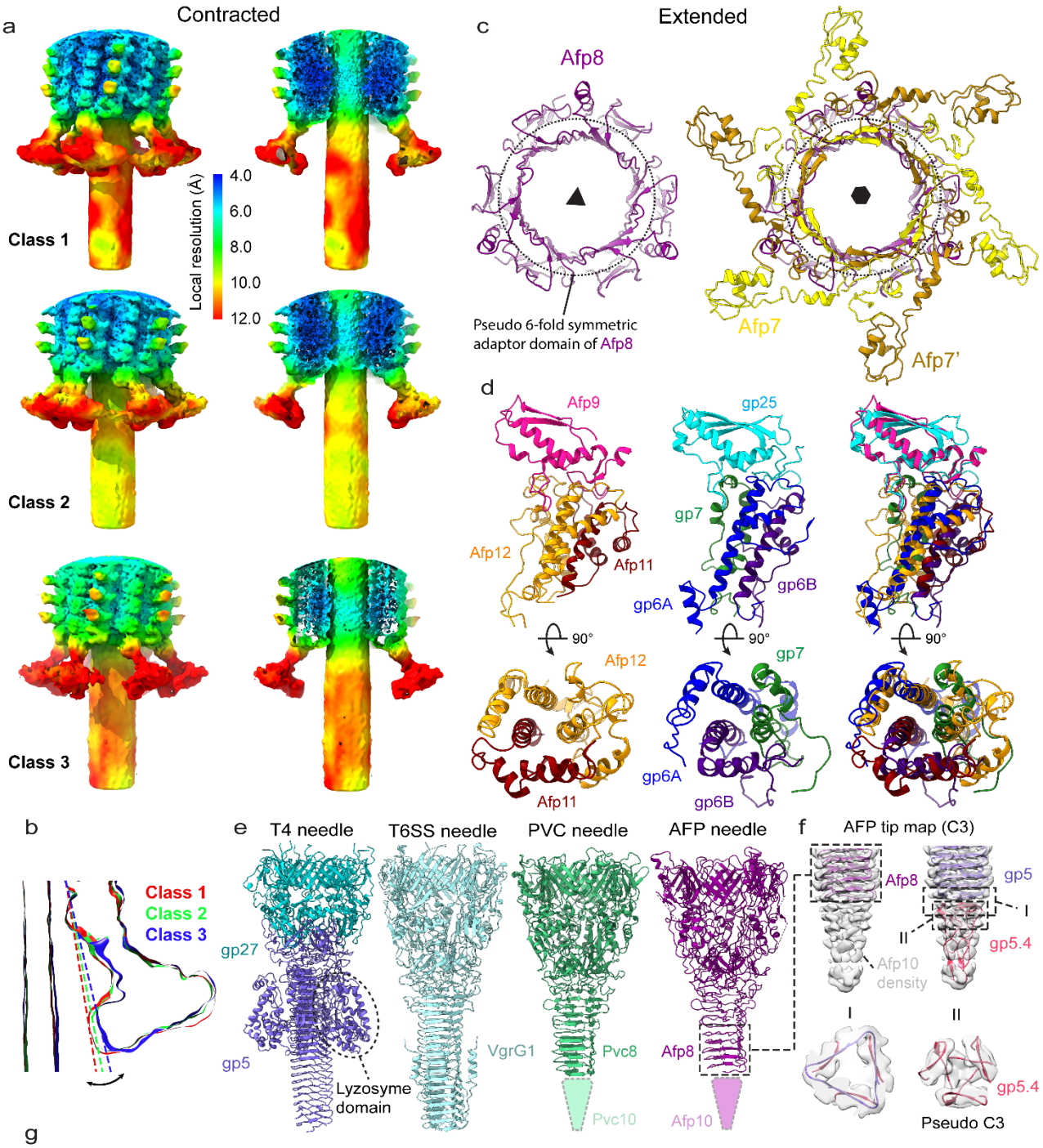
a
Contracted
Class 1
Class 2
Class 3
Local resolution (Å)
4.0
6.0
8.0
10.0
12.0
c
Extended
Afp8
Pseudo 6-fold symmetric adaptor domain of Afp8
Afp7
Afp7'
d
Afp9
Afp12
Afp11
gp25
gp7
gp6A
gp6B
90°
b
Class 1
Class 2
Class 3
e
T4 needle
T6SS needle
PVC needle
AFP needle
gp27
gp5
Lyzosyme domain
VgrG1
Pvc8
Pvc10
Afp8
Afp10
f
AFP tip map (C3)
Afp8
gp5
gp5.4
Afp10 density
I
II
Pseudo C3
g
Afp10 1 MSNLVVIDGDALTFNPQFGAITITPPPQPRISGSGEASIGGKKICIVGDEKQVSFTVDYIKPPFVAS-----PG 69
Pvc10 1 MSEAIVVDGDVLQFDPNFGNRQVTVPSPGKISGTGHAQVSGKKVCILGDEKQVRVSATYITTT-HTT-----PG 68
gp5.4 1 MSG--------LSYDKCVTAGHEAWPPTVVNATQSKVFTGGIAVLVAGDPITE---HTEIKKPYETHGGVTQPR 63
** * :: . : * : ... .* : : ** *. : *
Afp10 70 KGTLTIKALASEQRAEFATAPAPMIVVGSQFTTQFQPTTPAQDPQGKPDT-D-LSAVTGVGTFINSQSFVTAG 140
Pvc10 69 TGTITISALDAGQQALQCTSGAALIIKGQQFTAMFTPELPAMNNTVTPPQPDVTTPSSGKGRFITQQNFATVN 141
gp5.4 64 TSKVYVT----GKKAVQMADP---ISCGD-----------------------TVAQASSKVFIK-------- 97
...: :. ::* : * *. :. **.
Residues conserved between Afp10 and Pvc10
Residues conserved between Afp10, Pvc10 and gp5.4

Supplementary Figure 9: Structural description of the AFP baseplate and needle. (a) Cryo-EM maps of three classes of the contracted AFP baseplate after 3D classification, coloured according to local resolution. Overall resolution estimates are 5.4 Å, 5.9 Å and 7.3 Å for Class 1, 2 and 3 respectively (see also Extended Figure 3). (b) Cut-out views of maps for Class 1, 2 and 3 of the contracted AFP baseplate illustrate the variability of the position of the wedge formed by Afp9, Afp11 and Afp12 (c) Depiction of the switch between pseudo 6-fold (3-fold) symmetry found in the adaptor domain of Afp8 (purple) in the extended AFP needle, and the 6-fold symmetry of the preceding Afp7 ring, with alternating Afp7 monomers coloured yellow/orange. 3-fold and 6-fold rotation axes are annotated with black triangles and hexagons respectively. (d) Structural comparison (left and middle) and alignment (right) between the complex formed by Afp9 (violet), Afp11 (dark red) and Afp12 (orange), extracted from the extended AFP baseplate, and the complex formed by phage T4 proteins gp6A (dark blue), gp6B (purple), gp7 (green) and gp25 (light blue) extracted from the phage T4 pre-attachment baseplate-tail tube complex (PDB ID: 5IV5). (e) Structural comparison between the needle from phage T4 (formed by gp5, coloured dark blue, and gp27, coloured cyan), T6SS (formed by VgrG1, coloured light blue), PVC (formed by Pvc8 and Pvc10) and AFP (formed by Afp8 and Afp10, coloured purple). The lysozyme domain in gp5 is annotated by a black dotted oval. T4, T6SS and PVC needle structures are extracted from PDB ID 1WTH, 6H3L and 6J0M respectively. (f) Zoom showing the cryo-EM map for the tip end of AFP with fitted Afp8 (left) or gp5 and gp5.4 (right) from phage T4. Inset I: gp5 is fitted in the upper part of the AFP tip map, which displays C3 symmetry. Inset II: The lower part of the AFP tip map displays pseudo-C3 symmetry and contains fitted gp5.4 (PDB ID: 4KU0). (g) Sequence alignment between Afp10, Pvc10 and gp5.4. Residues conserved between Afp10, Pvc10 and gp5.4 are labelled red, while residues conserved between Afp10 and Pvc10 are labelled black.

Supplementary Tables

Supplementary Table 1. AFP proteins and their homologues

Afp Protein	MW (no. of amino acids)	Number of copies in extended AFP[1]	Location, function	Phage T4 homologue	T6SS homologue	R-type pyocin homologue	PVC homologue
Afp1	16.4 kDa (149)	126	Inner tube	gp19	Hcp	PA0623	Pvc1
Afp2	38.8 kDa (354)	66	Sheath	gp18	TssB/C, VipA/B	PA0622	Pvc2
Afp3	48.7 kDa (451)	60	Sheath	gp18	TssB/C, VipA/B	PA0622	Pvc3
Afp4	45.5 kDa (417)	6	Sheath	gp18	TssB/C, VipA/B	PA0622	Pvc4
Afp5	17.0 kDa (149)	6	Second layer of inner tube, tube initiator	gp54	Hcp	PA0623	Pvc5
Afp6	6.7 kDa (55)	Unknown[2]	Unknown	-	-	-	Pvc6
Afp7	25.2 kDa (229)	6	First layer of inner tube, tube initiator	gp48/gp53 LysM	Hcp	PA0623/PA0627 LysM	Pvc7
Afp8	58.0 kDa (529)	3	Baseplate, needle	gp5/gp27	VgrG	PA0616/PA0628	Pvc8
Afp9	15.7 kDa (140)	6	Baseplate, sheath initiator	gp25	TssE	PA0617	Pvc9
Afp10	14.5 kDa (140)	1	Baseplate, needle tip	gp5.4	VgrG PAAR	PA0616	Pvc10
Afp11	67.3 kDa (607)	6	Baseplate	gp6	TssF	PA0618	Pvc11
Afp12	106.8 kDa (963)	6	Baseplate	gp6/gp7	TssF/G	PA0619	Pvc12
Afp13	60.7 kDa (636)	6	Tail fibre protein	gp12	-	PA0620	Pvc13
Afp14	62.5 kDa (554)	Not present[3]	Tape measure protein	gp29	-	PA0625	Pvc14
Afp15	78.9 kDa (696)	Not present[3]	Chaperone/ATPase (predicted)	-	ClpV	-	Pvc15
Afp16	32.2 kDa (295)	6	Cap	gp15	TssA	PA0626	Pvc16
Afp17	40.5 kDa (358)	Not present[3]	Remnant toxin	-	-	-	-
Afp18	263.4 kDa (2366)	1[1,2]	Toxin	-	-	-	-

[1]Number of proteins fitted in the cryo-EM map of the major population of extended AFP (terminated by Afp2-Afp16), except for Afp18, which was estimated to be present as a single copy by mass spectrometry

[2]Detected by mass spectrometry but not localised in the cryo-EM map

[3]Not detected by mass spectrometry

Supplementary Table 2. Cryo-EM data collection, refinement and validation statistics

	Extended trunk (EMDB-4802) (PDB 6RBN)	Extended cap ending Afp2-Afp16 (EMDB-4784) (PDB 6RAP)	Extended cap ending Afp3-Afp16 (EMDB-4801)	Extended baseplate C6 (EMDB-4782) (PDB 6RAO)	Extended baseplate C3 (EMDB-4800) (PDB 6RBK)	Extended needle from subtracted images (EMDB-4781)	Contracted sheath C6/helical (EMDB-4803) (PDB 6RC8)	Contracted sheath C6 (EMDB-4859)	Contracted baseplate (EMDB-6RGL)
Data collection and processing									
Magnification	37,000x	37,000x	37,000x	37,000x	37,000x	37,000x	47,000x	47,000x	47,000x
Voltage (kV)	300	300	300	300	300	300	300	300	300
Electron exposure (e–/Å^2)	20	20	20	20	20	20	27	27	27
Defocus range (μm)	1.0-3.5	1.0-3.5	1.0-3.5	1.0-3.5	1.0-3.5	1.0-3.5	1.0-3.5	1.0-3.5	1.0-3.5
Pixel size (Å)	1.35	1.35	1.35	1.35	1.35	1.35	1.40	1.40	1.40
Symmetry imposed	C6, helical	C6	C6	C6	C3	C3	C6, helical	C6	C6
Initial particle images (no.)	30,858	30,858	30,858	46,991	46,991	46,991	15,189	15,189	30,378
Final particle images (no.)	30,858	23,797	7061	46,991	46,991	46,991	15,189	15,189	14,453
Map resolution (Å) FSC threshold	2.78 Å 0.143	3.2 Å 0.143	3.4 Å 0.143	3.1 Å 0.143	3.3 Å 0.143	3.7 Å 0.143	3.8 Å 0.143	4.2 Å 0.143	4.6 Å 0.143
Map resolution range (Å)	2.7-3.3 Å	3.0-4.2 Å	3.0-4.2 Å	2.9-4.2 Å	3.1-4.2 Å	3.4-5.0 Å	3.8-5.0 Å	4.0-6.0Å	4–12 Å
Refinement									
Initial model used (PDB code)	*de novo*	*de novo*	-	*de novo*	*de novo*	-	*de novo*	-	-
Model resolution (Å) FSC threshold	3.1 0.5	3.4 0.5	-	3.3 0.5	3.4 0.5	-	4.4 0.5	-	-
Model resolution range (Å)	∞ - 3.1	∞ - 3.4	-	∞ - 3.3	∞ - 3.4	-	∞ - 4.4	-	-
Map sharpening *B* factor (Å^2)	-92	-100	-95	-105	-102	-166	-260	-240	-270
Model composition Non-hydrogen atoms Protein residues Ligands	 7745 1004 0	 9879 1398 0	-	 22,409 3608 0	 7378 987 0	-	 5423 805 0	-	-
B factors (Å^2) Protein Ligand	 77 -	 55 -	-	 51 -	 46 -	-	 91 -	-	-
R.m.s. deviations Bond lengths (Å) Bond angles (°)	 0.0068 1.27	 0.0084 1.40	-	 0.0086 1.44	 0.0090 1.57	-	 0.0036 1.07	-	-
Validation MolProbity score Clashscore Poor rotamers (%)	 1.56 3 0.8	 1.82 5 1.5	-	 2.31 10 2.0	 2.17 5 1.7	-	 1.91 5 1.1	-	-
Ramachandran plot Favored (%) Allowed (%) Disallowed (%)	 92.9 6.8 0.3	 90.1 9.7 0.2	-	 87.6 11.8 0.6	 84.5 15.0 0.5	-	 87.6 12.4 0.0	-	-

Supplementary Table 3. Model refinement and validation statistics for individual Afp proteins

Protein	Afp1 (Afp2-bound)	Afp1 (Afp3-bound)	Afp1 (apical)	Afp1 (proximal)	Afp2	Afp2 (apical)	Afp2 (proximal)	Afp3	Afp4	Afp5	Afp7 (A)[1]	Afp7 (B)[1]	Afp8	Afp9	Afp11	Afp12	Afp16	Afp2 (contracted)	Afp2 (contracted, proximal)	Afp3 (contracted)	Afp4 (contracted)
PDB ID	6RBN	6RBN	6RAP	6RAO	6RBN	6RAP	6RAO	6RBN	6RAO	6RAO	6RBK	6RBK	6RBK	6RAO	6RAO	6RAO	6RAP	6RC8	6RGL	6RC8	6RGL
Map used for building[2]	ET	ET	EC	EB6	ET	EC	EB6	ET	EB6	EB6	EB3	EB3	EB3	EB6	EB6/EB3	EB6/EB3	EC	CS	CB	CS	CB
R.m.s deviations																					
Bond lengths (Å)	0.0071	0.0076	0.0106	0.0098	0.0068	0.0096	0.0084	0.0063	0.0096	0.0104	0.0088	0.0089	0.0086	0.0080	0.0087	0.0091	0.0083	0.0036	0.0118	0.0036	0.0107
Angles (°)	1.22	1.31	1.43	1.40	1.27	1.40	1.38	1.27	1.41	1.37	1.50	1.57	1.57	1.54	1.46	1.53	1.56	1.08	1.59	1.05	1.58
Validation																					
MolProbity score	1.69	1.44	2.24	1.68	1.61	1.58	1.88	1.56	2.47	1.77	1.83	2.19	1.97	2.21	1.98	2.19	2.24	2.03	2.60	1.89	2.47
Clashscore	5.28	2.20	7.86	3.96	3.37	2.26	5.80	3.29	11.99	4.58	3.78	4.91	4.49	6.02	5.85	6.88	11.14	4.90	14.53	4.98	17.82
Rotamer outliers (%)	0.00	0.00	3.12	0.00	0.35	0.71	1.06	0.68	2.50	0.00	0.00	2.11	1.19	2.78	0.55	1.33	0.85	1.77	2.13	0.00	2.13
C-beta outliers	0	0	0	0	0	0	1	0	3	0	0	0	0	0	0	0	1	0	0	0	0
Ramachandran																					
Favoured (%)	93.84	93.15	93.20	91.78	92.24	88.76	89.97	93.18	88.95	90.48	85.07	83.33	93.27	90.08	84.86	81.16	84.27	88.44	83.53	86.82	85.79
Allowed (%)	5.48	5.48	6.80	6.85	7.76	11.24	9.74	6.82	10.79	9.52	14.93	16.22	16.13	6.61	14.92	18.47	15.73	11.56	46.47	13.18	13.68
Disallowed (%)	0.68	1.37	0.00	1.37	0.00	0.00	0.29	0.00	0.26	0.00	0.00	0.45	0.60	3.31	0.22	0.37	0.00	0.00	0.00	0.00	0.00
Amino acids built/total amino acids (%)	148/149 (99.3%)	148/149 (99.3%)	149/149 (100%)	148/149 (99.3%)	350/354 (98.9%)	349/354 (98.6%)	351/354 (99.2%)	359/451 (79.6%)	386/417 (92.6%)	149/149 (100%)	224/229 (97.8%)	223/229 (97.3%)	504/529 (95.3%)	125/140 (89.3%)	465/607 (76.6%)	546/963 (56.7%)	276/295 (93.6)	348/354 (98.3%)	348/354 (98.3%)	355/451 (78.7%)	386/417 (92.6%)

[1]Afp7 (A) and (B) correspond to adjacent (but non symmetry-related) copies of Afp7 in the 3-fold symmetrised baseplate

[2]ET = extended trunk, EC = extended cap (ending Afp2-Afp16), EB6 = extended baseplate C6, EB3 = extended baseplate C3, CS = contracted sheath (helical), CB = contracted baseplate

Supplementary Table 4. Interaction energy and buried surface area between extended AFP needle, tube and cap subunits

Interaction	ΔG, kcal/mol	Buried Surface Area, Å^2	Description
Afp8-Afp7	-19.6	1568.8	Value for 1x Afp8 + 4x Afp7
Afp7-Afp5	-12.0	859.9	Value for 1x Afp5 + 2x AFp7
Afp5-Afp1	-17.2	1087.9	Value for 1x Afp5 + 4x Afp1
Afp1-Afp1	-22.7	1325.8	Value for 1x Afp1 in one layer with 4x Afp1 from adjacent layers
Afp1-Afp16	-20.7	1594.0	Value for 1x Afp16 + 3x Afp1

Supplementary Table 5. Comparison of AFP, R-pyocin and T6SS state tube-tube, sheath-sheath and tube-sheath interaction energies

Interaction	AFP ΔG, kcal/mol	R-Pyocin ΔG, kcal/mol	T6SS ΔG, kcal/mol
Tube-sheath	-4.2	-1.4	-3.3
Tube-tube	-51.9	-49.0	-49.1
Sheath-sheath (extended)	-105.2	-57.5	-129.4
Sheath-sheath (contracted)	-111.0	-68.0	-161.2
Contracted and extended sheath-sheath difference	**-5.8**	**-10.5**	**-31.8**

Supplementary Table 6. Interaction energies and buried surface areas between Afp2 and Afp3 subunits for extended and contracted AFP sheath

Interaction	Extended state			Contracted state		
	ΔG, kcal/mol	Contribution to total	Buried surface area, Å^2	ΔG, kcal/mol	Contribution to total	Buried surface area, Å^2
Afp2 C-ter-Afp3 C-ter (layer n-1)	-27.4	26%	1417.4	-26.6	24%	1529.5
Afp2 C-ter-Afp3 C-ter (layer n+1)	-30.0	29%	1613.1	-25.6	23%	1559.6
Afp2 C-ter-Afp3 N-ter (layer n+1)	-10.9	10%	691.5	-10.5	9%	531.4
Afp2 N-ter-Afp2 C-ter (layer n)	-12.4	12%	617.0	-11.3	10%	554.7
Afp2 N-ter-Afp3 C-ter (layer n-1)	-10.6	10%	649.6	-10.1	9%	640.1
Afp3 N-ter-Afp3 C-ter (layer n)	-13.9	13%	657.4	-11.1	10%	569.2
Afp2-Afp2 (layers n+2/n-2)	-	-	-	-7.4	7%	567.7
Afp3-Afp3 (layers n+2/n-2)	-	-	-	-8.4	8%	587.7
TOTAL	**-105.2**	**100%**	**5646.0**	**-111.0**	**100%**	**6539.9**